Available online at www.sciencedirect.com
ScienceDirect
Journal of Solid State Chemistry 180 (2007) 3253–3261
JOURNAL OF SOLID STATE CHEMISTRY
www.elsevier.com/locate/jssc

Electronic state of ^{57}Fe used as Mössbauer probe in the perovskites $LaMO_3$ (M = Ni and Cu)

Igor Presniakov[a], Gérard Demazeau[b,*], Alexei Baranov[a,b], Alexei Sobolev[a], Tatyana Gubaidulina[a], Viyacheslav Rusakov[a]

[a]*Lomonosov Moscow State University, 119992 Leninskie Gory, Moscow, Russia*
[b]*ICMCB, CNRS, University BORDEAUX 1 "Sciences and Technologies", site de l'ENSCPB-87, Avenue du Dr A. Schweitzer, 33608 PESSAC Cedex, France*

Received 9 July 2007; received in revised form 13 September 2007; accepted 15 September 2007
Available online 21 September 2007

Abstract

For the first time a comparative study of rhombohedral $LaNiO_3$ and $LaCuO_3$ oxides, using ^{57}Fe Mössbauer probe spectroscopy (1% atomic rate), has been carried out. In spite of the fact that both oxides are characterized by similar crystal structure and metallic properties, the behavior of ^{57}Fe probe atoms in such lattices appears essentially different. In the case of $LaNi_{0.99}Fe_{0.01}O_3$, the observed isomer shift (δ) value corresponds to Fe^{3+} ($3d^5$) cations in high-spin state located in an oxygen octahedral surrounding. In contrast, for the $LaCu_{0.99}Fe_{0.01}O_3$, the obtained δ value is comparable to that characterizing the formally tetravalent high-spin Fe^{4+}($3d^4$) cations in octahedral coordination within Fe(IV) perovskite-like ferrates. To explain such a difference, an approach based on the qualitative energy diagrams analysis and the calculations within the cluster configuration interaction method have been developed. It was shown that in the case of $LaNi_{0.99}Fe_{0.01}O_3$, electronic state of nickel is dominated by the d^7 configuration corresponding to the formal ionic "Ni^{3+}–O^{2-}" state. On the other hand, in the case of $LaCu_{0.99}Fe_{0.01}O_3$ a large amount of charge is transferred via Cu–O bonds from the O:2p bands to the Cu:3d orbitals and the ground state is dominated by the $d^9\underline{L}$ configuration ("$Cu^{2+}-O$" state). The dominant $d^9\underline{L}$ ground state for the (CuO_6) sublattice induces in the environment of the ^{57}Fe probe cations a charge transfer $Fe^{3+} + O^-(\underline{L}) \rightarrow Fe^{4+} + O^{2-}$, which transforms "$Fe^{3+}$" into "$Fe^{4+}$" state. The analysis of the isomer shift value for the formally "Fe^{4+}" ions in perovskite-like oxides clearly proved a drastic influence of the 4s iron orbitals population on the Fe−O bonds character.

Keywords: Ni^{3+} and Cu^{3+} perovskites; ^{57}Fe Mössbauer probe; Mössbauer study; Charge transfer

1. Introduction

The majority of physical properties of inorganic compounds containing transition-metal ions depend closely on the formal oxidation state and the electronic configuration that they adopt in the material. The oxidation state (m) of a transition metal M^{m+} is a formal number reflecting the average number of d electrons involved in chemical bonding. Its stability is not only an intrinsic atomic property (energy of ionization, electronegativity and electron repulsion parameters, etc.) but it closely depends also both on local structural factors (ionic size, local symmetry of the site, etc.) and on chemical factors (covalency, influence of competing bonds, etc.) A preliminary study [1], based on Tanabe–Sugano diagrams [2] and calculations of the energy levels corresponding to the d orbitals versus the local distortion [3], has underlined that the stabilization of a specific electronic configuration of the transition-metal ion M^{m+}: d^n ($1<n<9$) can be related to two factors. The first is the axial distortion parameter $\theta = d_{||}/d_{\perp}$ equal to the ratio of the metal-ligand distance $M^{m+}-O$ ($d_{||}$) along the fourfold axis, to that ($d_{\perp}$) in the perpendicular plane. The second concerns the local crystal field energy Dq/B correlated to the chemical bonding of such a d^n cation (Dq and B are the crystal field and Racah parameters, respectively). This simple approach demonstrated how a good agreement between

*Corresponding author. Fax: +33 5 40 00 27 10.
E-mail address: demazeau@icmcb.u-bordeaux1.fr (G. Demazeau).

0022-4596/$ - see front matter © 2007 Elsevier Inc. All rights reserved.
doi:10.1016/j.jssc.2007.09.016

the above-mentioned factors and a given electronic configuration might help the stabilization of unusual oxidation states.

The above arguments have been applied to the synthesis of perovskite-like iron oxides containing six-coordinated Fe^{4+} and Fe^{5+} ions [4]. The first stoichiometric Fe(IV) oxides prepared under oxygen pressure have been $SrFeO_3$ and $CaFeO_3$ [5,6]. In the $SrFeO_3$ ferrate, due to the O_h symmetry of the (FeO_6) octahedra and the strong covalency of the Fe–O bonds, metallic behavior was observed [7]. Another example is the bidimensional (2D) Fe(IV) oxides $La_{1.5}M_{0.5}Li_{0.5}Fe_{0.5}O_4$ (M = Ca, Sr, Ba) [8] with the K_2NiF_4 structure, suitable for favoring an elongation (D_{4h} symmetry) of the (FeO_6) octahedra. To increase the local tetragonal distortion and to isolate the high-spin $Fe^{4+}(t_{2g}^3e_g^1)$ ions ($^5A_{1g}$ ground term) from each other's, the presence of relatively ionic Li–O competing bonds within the perovskite layers also appeared to be appropriated. The use of similar arguments has led to the synthesis of the 3D perovskite La_2LiFeO_6 containing six-coordinated Fe^{5+} ions with a highly isotropic electronic configuration $t_{2g}^3e_g^0$ ($^4A_{2g}$ ground term) [9].

^{57}Fe Mössbauer spectroscopy, owing to the high resolution on energy, allows not only to define the oxidation state of the iron atoms but also to get important informations on their local surrounding (crystallographic environment, chemical bonding and electronic structure). In particular, Mössbauer studies of $CaFeO_3$ revealed a charge disproportionation $2Fe^{4+} \rightarrow Fe^{3+} + Fe^{5+}$ at $T_t \leqslant 250$ K [10]. A study of the hyperfine parameters as a function of temperature has shown that this process occurs in varying degrees (σ), resulting in the charge states $Fe^{(4-\sigma)+}$ and $Fe^{(4+\sigma)+}$ [11]. Such a disproportionation has also been observed in the related ternary phases $Sr_{1-x}Ca_xFeO_3$ [12], $SrFe_{1-x}Co_xO_3$ [13] and $La_{1-x}A_xFeO_3$ (A = Ca, Sr) [14]. Mössbauer studies of these ferrates have revealed a suitable dependence between the relative strengths of the Fe(e_g)–O(p_σ)–Fe(e_g) interactions and the electron–phonon coupling for the disproportionation reaction occurs. When the Fe–O–Fe interactions are stronger, as appears to be the case of $SrFeO_3$ ferrate which give metallic conductivity to the lowest temperatures, the quarter-filled σ^{*1} band of itinerant electrons does not lead to disproportionation [12].

Besides the Fe(IV) ferrates, the above considerations seems to be operative in many other materials containing the JT ions. For example, nickelates $RNiO_3$ (R = rare-earth, Y, Tl) containing low-spin $Ni^{3+}(t_{2g}^6e_g^1)$ ions [15,16]. Recently carried out theoretical investigation [17] has shown, that the charge ordering (disproportionation or charge density wave) may occur in a crossover between localized and itinerant regimes, if an intra-atomic Hund's exchange energy (J_H) overcomes the on site Coulomb repulsion energy (U).

Due to the limited number of chemical compounds containing Mössbauer isotopes, a probe variant of the Mössbauer spectroscopy was developed—such a method consisted on the analysis of hyperfine interaction parameters of the probe atoms (^{57}Fe, ^{119}Sn) participating to the structure of studied compounds. Recently, this method has been applied to characterize the electronic phenomena (orbitals ordering, charge disproportionation, insulator-metal transition) in perovskite-like Ni(III) nickelates $RNi_{0.99}Fe_{0.01}O_3$ [18–20]. It has been shown that Mössbauer spectra of ^{57}Fe probe atoms reflect structural and chemical factors characterizing not only their local environment but also the electronic phenomena involving the bulk.

The objectives of this work are to characterize the electronic state and local surrounding of ^{57}Fe Mössbauer probe atoms within iron-doped perovskites $LaNiO_3$ and $LaCuO_3$ lattices containing transition-metal ions in unusual formal oxidation states "+3".

$LaNiO_3$ was prepared a long time ago by different authors using normal pressure conditions [21–23]. On the other hand the synthesis of $LaCuO_3$ required high oxygen pressures [24].

The electronic structure of the Jahn–Teller $Ni^{3+}(t_{2g}^6e_g^1)$ and $Cu^{3+}(t_{2g}^6e_g^2)$ ions has attracted great interest because it remains to be clarified whether their ground states, due to the strong covalency of the M^{3+}–O bond (M = Ni, Cu), are dominated by $d^7(Ni^{3+})$ and $d^8(Cu^{3+})$ or $d^8\underline{L}$ ("$Ni^{2+}-O^-$" state) and $d^9\underline{L}$ ("Cu^{2+}–O^-" state), where $\underline{L}$ is an oxygen hole. A comparative study of these rhombohedral perovskites (both oxides being characterized by Pauli paramagnetism [24,25]) had evidenced that the differences between the magnitudes and thermal evolutions of their respective susceptibilities could be explained in terms of antiferromagnetic vs. ferromagnetic superexchange enhancement and large vs. small spin polarons associated with the excited states [26].

A first Mössbauer study using ^{57}Fe as doping probe was published early but using the non-stoichiometric matrix $LaCuO_{3-x}$ with the tetragonal structure contaminated by few amounts of CuO and $LaFeO_3$ [27]. Subtracting the contamination by $LaFeO_3$, the remaining spectrum was analyzed using three contributions attributed to high spin Fe^{3+}, intermediate spin Fe^{3+} or Fe^{4+}. Such contaminations impeded a correct interpretation of ^{57}Fe Mössbauer spectra.

2. Experimental

Polycrystalline sample of $LaCuO_3$ doped with about 1 at% ^{57}Fe ($LaCu_{0.99}{}^{57}Fe_{0.01}O_3$) has been prepared under an oxygen atmosphere of 11.5 GPa at 900 °C < T < 950 °C in a belt-type apparatus, using $KClO_3$ as in situ oxygen source. Details of preparation and characterization of $LaCuO_3$ doped by ^{57}Fe Mössbauer probe are published elsewhere [28].

In order to synthesize $LaNi_{0.99}Fe_{0.01}O_3$, NiO: ^{57}Fe (1%) oxide was obtained through the annealing of the coprecipitated hydroxides at 350 °C under inert argon atmosphere. In the case of $LaNiO_3$ doped with ^{57}Fe (1%), the preparation process was operating through solid state

reactions in two steps: firstly, $La_2O_3 + 2NiO$: ^{57}Fe under gas O_2 pressure 100 MPa at 900 °C, and secondly, with 15% $KClO_3$ (referred to the total weight of the precursors) as in situ oxygen source under 2 GPa, 900 °C, 5 min, in order to be sure for the insertion of the Mössbauer probe into the lattice ($LaCu_{0.99}Fe_{0.01}O_3$), and for the oxygen stoichiometry equal 3. Oxygen stoichiometry was defined through oxido–reduction titration.

X-ray diffraction (XRD) data were collected at 298 K using a STOE diffractometer (Cu$K\alpha$ radiation).

The ^{57}Fe Mössbauer spectra were recorded at 300 K using a conventional constant-acceleration spectrometer. The radiation source $^{57}Co(Rh)$ was kept at room temperature. All isomer shifts refer to the α-Fe absorber at 300 K.

2.1. Structural characterization of the $LaM_{0.99}{}^{57}Fe_{0.01}O_3$ (M = Ni, Cu) samples

The XRD patterns (using K_α(Cu), $\lambda = 1.5451$ Å) given on Fig. 1 underline that all diffraction peaks for both $LaM_{0.99}{}^{57}Fe_{0.01}O_3$ oxides (M = Ni, Cu) can be indexed in the frame of the rhombohedral crystal lattice (space group $R\bar{3}c$). The indexation (hexagonal cell) of the XRD peaks is given in Table 1. The calculated cell parameters for the

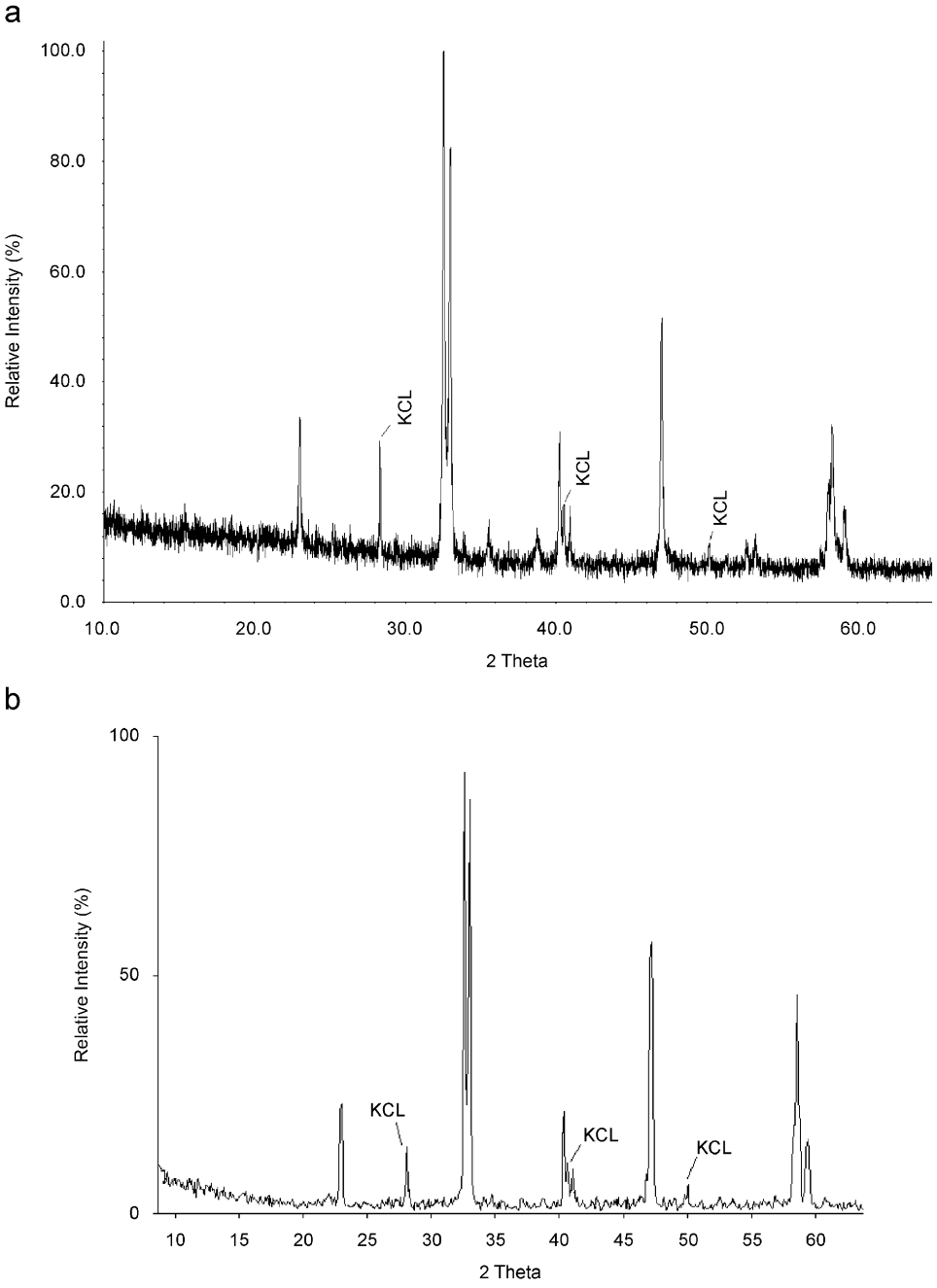

Fig. 1. Powder X-ray diffraction profiles of iron-doped $LaNiO_3$ and $LaCuO_3$ samples.

Table 1
X-ray diffraction data for $LaM_{0.99}{}^{57}Fe_{0.01}O_3$ (M = Ni, Cu) samples

$LaNi_{0.99}{}^{57}Fe_{0.01}O_3$($R\bar{3}c$)					$LaCu_{0.99}{}^{57}Fe_{0.01}O_3$ ($R\bar{3}c$)				
d	h	k	l	I, %	d	h	k	l	I, %
3.864(5)	0	1	2	33.52	3.862(9)	0	1	2	36.41
2.750(5)	1	1	0	100.0	2.748(2)	1	1	0	100.0
2.715(1)	1	0	4	97.10	2.714(4)	1	0	4	94.23
2.333(1)	1	1	3	12.11	2.322(0)	1	1	3	13.76
2.240(9)	2	0	2	20.82	2.239(7)	2	0	2	29.94
2.202(8)	0	0	6	15.85	2.202(4)	0	0	6	16.47
1.932(3)	0	2	4	53.16	1.931(2)	0	2	4	51.90
1.737(3)	1	2	2	8.65	1.737(5)	1	2	2	10.65
1.719(4)	1	1	6	13.54	1.719(0)	1	1	6	13.14
1.588(0)	3	0	0	17.21	1.598(2)	3	0	0	19.67
1.581(1)	2	1	4	32.63	1.580(2)	2	1	4	32.26
1.560(9)	0	1	8	15.02	1.560(1)	0	1	8	16.11
$a = b = 5.501$ Å, $c = 13.21_7$ Å, $V = 346.4$ Å^3, $c/a = 2.402$					$a = b = 5.498$ Å, $c = 13.21_1$ Å, $V = 345.8$ Å^3, $c/a = 2.403$				

$LaNi_{0.99}Fe_{0.01}O_3$ ($a = b = 5.501$ Å, $c = 13.21_7$ Å) and $LaCu_{0.99}Fe_{0.01}O_3$ ($a = b = 5.498$ Å, $c = 13.21_1$ Å) are close to that observed, respectively for the undoped perovskites: $LaNiO_3$ ($a = b = 5.459$ Å, $c = 13.13_1$ Å) [22] and $LaCuO_3$ ($a = b = 5.501$ Å, $c = 13.21_7$ Å) [24,29,30]. Such a result can be attributed to the small atomic rate of the ^{57}Fe Mössbauer probe atoms (1%) into the investigated matrixes in spite of the different ionic sizes: $r(Fe^{3+}) = 0.64$ Å, $r(Ni^{3+}) = 0.54$ Å, $r(Cu^{3+}) = 0.55$ Å [31].

3. Results and discussion

The ^{57}Fe Mössbauer spectra of the $LaM_{0.99}{}^{57}Fe_{0.01}O_3$ (M = Ni, Cu) samples measured at $T = 300$ K (see Fig. 2) can be described as a single not resolved quadrupole doublet. The ^{57}Fe Mössbauer parameters corresponding to the both perovskites are given in Table 2. The full linewidth at half height (Γ) for each component of doublets was found to be close to the corresponding value for the calibration spectrum ($\Gamma = 0.27$ mm/s), which is evidence of only one type of the crystallographic position is occupied by the dopant ^{57}Fe atoms in the both perovskites.

The small values of the quadrupole splitting (Δ) for the doublets (Table 2) are consistent with the nearly non-distorted octahedral (NiO_6) and (CuO_6) polyhedra in the both considered matrix resulting from the itinerant character of the e_g electron(s) (σ^* band) in the $LaNiO_3$ (Ni^{3+}: $t_{2g}^6\sigma^{1*}$) and the $LaCuO_3$ (Cu^{3+}: $t_{2g}^6\sigma^{2*}$) [26].

The significant difference of the isomer shifts (δ) values for the doublets could be attributed to a distinction of the valence states for the iron cations in the considered matrixes. For $LaNi_{0.99}Fe_{0.01}O_3$, the obtained δ value corresponds to the Fe^{3+} ($3d^5$) cations in high-spin state located in the oxygen octahedral surrounding [32]. In the case of $LaCu_{0.99}Fe_{0.01}O_3$, the δ value is in a range of the corresponding values $-0.12+/-0.02$ mm/s, typical for tetravalent Fe^{4+}($3d^4$) cations in the perovskite-like oxides [32].

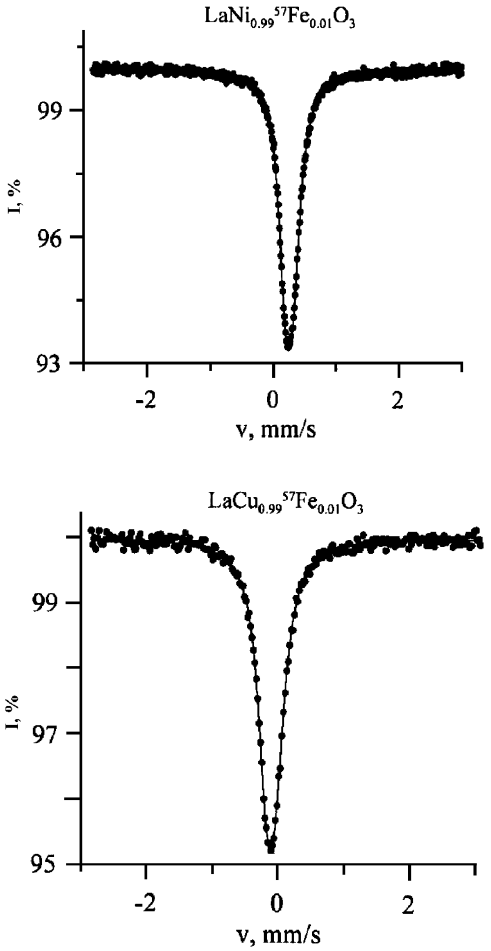

Fig. 2. ^{57}Fe Mössbauer spectra of $LaM_{0.99}{}^{57}Fe_{0.01}O_3$ (M = Ni, Cu) at $T = 300$ K.

The main interest for the discussion of these results is the mechanism responsible for the stabilization of two different

^{57}Fe charge states in the $LaM_{0.99}{}^{57}Fe_{0.01}O_3$ (M = Ni, Cu) matrixes. This discussion is started with a summary of the relevant features of the electronic structure for $LaNiO_3$ and $LaCuO_3$ perovskites. Fig. 3 represents schematically the steps used for the construction of a band diagram for these compounds starting from an ionic model, which was applied to 3d transition-metal oxides by Torrance [33]. Fig. 3 (point charge approximation) shows octahedral-site $Ni^{4+/3+}$, $Cu^{4+/3+}$ and $Fe^{4+/3+}$ (impurity) redox energies (ε), which are given by

$$\varepsilon(M^{3+/4+}) = -I_4 - eV_{Mad}, \quad (1)$$

where I_4 is the fourth ionization potential [34]; V_{Mad} is the Madelung potential acting on the M^{3+} ion (for V_{Mad} calculation we used crystallographic data for $LaNiO_3$ [22] and $LaCuO_3$ [24,29,30] lattices).

The lowest unoccupied $M^{3+/2+}$ (=Ni, Cu) redox level lies at an energy U_0 above the highest occupied $M^{4+/3+}$ level, as shown in Fig. 3 (point charge approximation). The $O^{2-/-}$ and $M^{3+/2+}$ levels are separated by the energy Δ_0, which corresponds to the charge transfer ($O^{2-} \rightarrow M^{3+}$) gap in the Zaanen–Sawatzky–Allen (ZSA) model [35]. The subscripts "zero" on U_0 and Δ_0 have been introduced to remind that these values are calculated using the simple ionic model. Corresponding values of U_0 and Δ_0 are given by the following expressions:

$$U_0 = I_4 - I_2 - e^2/d_{M\text{-}M}, \quad (2a)$$

$$\Delta_0 = -I_3 - A(O^-) + e\Delta V_M - e^2/d_{M\text{-}O}, \quad (2b)$$

where $\Delta V_M[= V_{Mad}(M^{3+}) - V_{Mad}(O^{2-})]$ is the difference in the Madelung potential between the metal M^{3+} site and the oxygen O^{2-} site; $A(O^-)$ is the electron affinity of O^- ion ($A(O^-) = 8$ eV [34]); e^2/d_{M-M} and e^2/d_{M-O} are the electrostatic terms including the electron–hole binding energies (d_{M-M} and d_{M-O} are the nearest-neighbor metal–metal and metal–oxygen distances, respectively).

The U_0 and Δ_0 values thus obtained for the Ni^{3+} ($U_0 = 16.0$ eV, $\Delta_0 = 10.7$ eV) are larger than for the Cu^{3+} ($U_0 = 14.6$ eV, $\Delta_0 = 8.4$ eV) ions which is consistent with the general tendency that the electron correlation becomes stronger as the atomic number of M^{m+} increases. Nevertheless, the U_0 and Δ_0 values have been calculated without any of the effects of the polarization of the constituent ions and the covalency in the M–O chemical bonds and are therefore expected to overestimate the actual parameter values. The polarization (ΔE_{pol}) raises energy of the filled $M^{3+/4+}$ level and approximately on the same value lowers energy of the lowest unoccupied $M^{3+/2+}$ (Fig. 3). The polarization corrections in $LaNiO_3$ ($\Delta E_{pol}(Ni) = 4.15$ eV) and $LaCuO_3$ ($\Delta E_{pol}(Cu) = 4.06$ eV) were taken into account by means of a technique developed by Zaanen and Sawatzsky [36]. The hybridization between the M:3d and O:2p orbitals weakens the localized nature of 3d electrons, and hence reduces electron correlations. However, the effect of covalency appears to be well corrected by

Table 2
^{57}Fe Mössbauer parameters for $LaM_{0.99}{}^{57}Fe_{0.01}O_3$ (M = Ni, Cu)

Compound	δ, mm/s	Δ, mm/s	Γ, mm/s
$LaNi_{0.99}Fe_{0.01}O_3$	0.26 (1)	0.12(1)	0.27(1)
$LaCu_{0.99}Fe_{0.01}O_3$	−0.11(1)	0.11(1)	0.28(1)

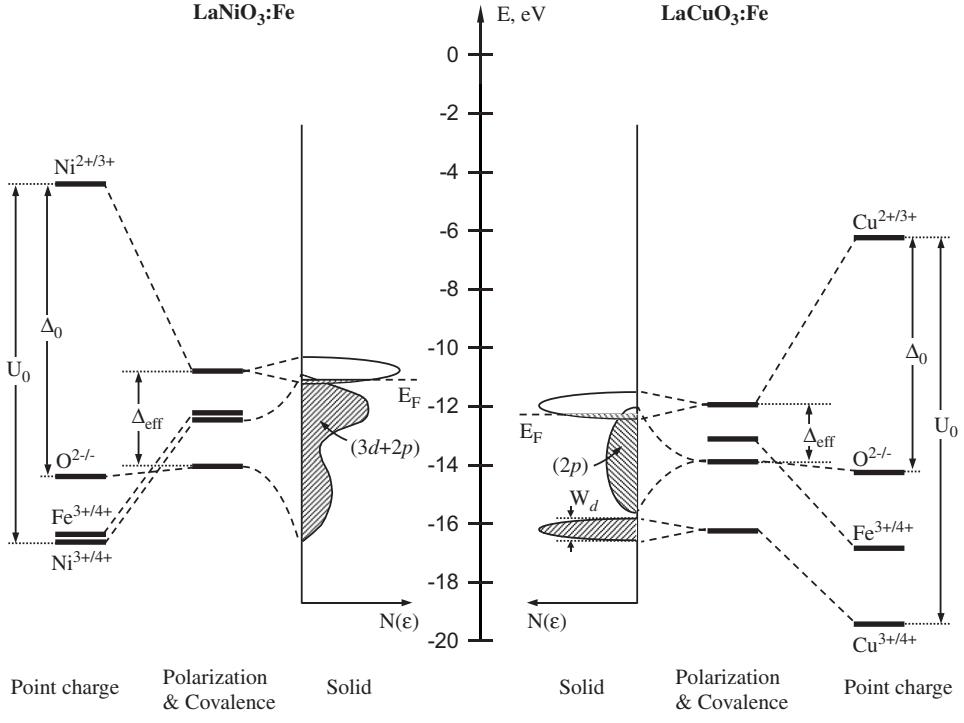

Fig. 3. Schematic representation of various steps in the construction of a band diagram for iron-doped $LaNiO_3$ and $LaCuO_3$ perovskites.

subtracting the constant term from the calculated U_0 and Δ_0 values irrespective of the M^{m+} species as shown in Fig. 3. Thus this simple ionic model seems to be a very good starting point to understand the reason of the observed different valence states for the iron cations in these oxides.

A comparison of the diagrams in Fig. 3 shows that $\varepsilon(Cu^{2+/3+}) \approx \varepsilon(Ni^{2+/3+}) \gg \varepsilon(Fe^{3+/4+})$. It means that, on the basis of the Ni^{2+}/Fe^{3+} and Cu^{2+}/Fe^{3+} energy levels, the electron-transfer equilibriums:

$$Ni^{3+} + Fe^{3+} \leftrightarrow Ni^{2+} + Fe^{4+}, \quad (3a)$$

$$Cu^{3+} + Fe^{3+} \leftrightarrow Cu^{2+} + Fe^{4+}, \quad (3b)$$

are evidently biased to the left. Thus, an oxidation of originally trivalent Fe^{3+} by the isovalent copper cations with a formal oxidation state "+3" (for which ones such state is very untypical) cannot cause the appearance of the higher-charge state Fe^{4+} in the $LaCu_{0.99}Fe_{0.01}O_3$ structure.

The most drastic difference of diagrams of the energy levels corresponding to discussed oxides concerns a relative arrangement of energy levels $\varepsilon(O^{2-/-})$ and $\varepsilon(M^{3+/4+})$, which influences on the covalence degree of the *M*–O bonds. In both cases the energies $\varepsilon(M^{3+/4+})$ and $\varepsilon(O^{2-/-})$ are close to each other that indicates a large covalency in the Ni–O and Cu–O bonds with a strong hybridization between O:2*p* and *M*:3*d* states. However, in the case of $LaNiO_3$ the ΔE_{pol}(Ni) correction causes the $Ni^{3+/4+}(3d^7)$ redox energy to cross the $O^{2-/-}$ redox energy, which is a necessary condition for an "ionic model" to be valid. The top of the valence band in $LaNiO_3$ is predominantly nickel in origin; however, there is significant admixture of 2*p* orbitals of oxygen (Fig. 3). On the contrary, in the case of $LaCuO_3$, the Madelung energy (eV_{Mad}) and the ΔE_{pol}(Cu) correction are not strong enough to raise the $Cu^{3+/4+}$ redox level above the $O^{2-}:2p^6$ level; the $Cu^{3+/4+}$ couple lies below the top of the O:2*p* band, so an oxidation of the "CuO_6" sub-lattice should introduce holes into the σ^* antibonding states pinned at the top of the valence O:$2p_\sigma$ band. In other words, representation of the ground-state properties of $LaCuO_3$ requires introduction of a strong hybridization of O:$2p_\sigma$ and Cu:$3d_\sigma$ orbitals in the itinerant-electron σ*–band states corresponding to an equilibrium charge transfer reaction:

$$Cu^{3+}(d^8) + O^{2-} \leftrightarrow Cu^{2+}(d^9) + O^-(\underline{L}), \quad (4)$$

that is biased strongly to the right. It is necessary to note that the $LaNiO_3$ oxide containing Ni^{3+} ions also is very covalent, though the extent of covalency in this compound is less pronounced than in the case of Cu^{3+}.

To obtain greater insight into the effects of covalency mentioned above we used a simple approximation of the Anderson impurity model [37]. The basis assumption in this model is that the ground state of transition metal $M^{m+}:d^n$ can be described as a mixture of the purely ionic state $|d^n\rangle$ and charge-transfer states $|d^{n+1}\underline{L}\rangle$, $|d^{n+2}\underline{L}^2\rangle$ in which one or two electrons are transferred to the 3*d* orbitals of M^{m+} ion from neighboring O:2*p* orbitals. The corresponding ground-state wave function (Ψ_g) for the transition metal ion is presented as a linear combination of the above multi-electronic configurations:

$$\Psi_g = \alpha_0|d^n\rangle + \beta_0|d^{n+1}\underline{L}\rangle \quad (\alpha_0^2 + \beta_0^2 \approx 1), \quad (5)$$

where for simplicity mixing with $|d^{n+2}\underline{L}^2\rangle$ state has been neglected. The configuration mixing coefficients α_0 and β_0 are related to each other in the following way [38]:

$$\frac{\beta_0}{\alpha_0} = \frac{(\Delta^2 + 4T^2)^{1/2} - \Delta}{2T}, \quad (6)$$

where *T* is an overlap integral of the multielectronic states. Energy of the charge transfer $\Delta = [E(d^n) - E(d^{n+1}\underline{L})]$, entering into this equation, differs from the one-electron energy Δ_0, calculated in the frames of ionic model described above. After the substitution for Δ and *T* parameters in Eq. (6) by the values received before from the XPS spectra of oxides, containing the Ni^{3+} ($\Delta = 1$ eV and $T_\sigma = 2.59$) [39] and Cu^{3+} ($\Delta = -1$ eV and $T_\sigma = 2.94$) [40] cations, the values of α_0 and β_0 coefficients were estimated, the second degrees of which ones are proportional to contributions of corresponding electronic states, (d^7 and $d^8\underline{L}$) and (d^8 and $d^9\underline{L}$), in wave function [expression (5)] for the Ni^{3+} and Cu^{3+} cations, respectively.

The obtained results evidence that, in case of $LaNi_{0.99}Fe_{0.01}O_3$ [61% (d^7) and 39% (d^8L)], the electronic state of nickel is preferentially described by d^7 configuration corresponding to the "ionic" pair Ni^{3+}–O^{2-}. On the contrary, for $LaCu_{0.99}Fe_{0.01}O_3$ [34% (d^8) and 66% (d^9L)], the basic state of the copper cations corresponds to an electronic configuration $d^9\underline{L}$ (Cu^{2+}–O^-). In that case, it is possible to assume that the probe Fe^{3+} cations introduced into the bulk of the $LaCuO_3$ lattice will appear in an anionic environment "$O^{(2-\sigma)-}$" with lower value of a negative charge. As electronegativity of oxygen sharply increases within downturn of its negative charge [41], the Fe–O bonds will be characterized by a very high ionicity degree that can be possible to present schematically as a displacement of the following reaction balance:

$$Cu^{2+} - O^-(\underline{L}) - Fe^{3+} \rightarrow Cu^{2+} - O^{2-} - Fe^{4+}. \quad (7)$$

Such a result is in agreement with the study of the electronic structure of formally Cu^{3+} into the $LaCuO_3$ matrix using photoemission and X-ray-absorption spectroscopy indicating that the ground state is dominated by the $d^9\underline{L}$ configuration [42–44]. The charge-transfer phenomenon had been also pointed out through "*ab initio*" calculations of the electronic structure based on the A.S.W. method [45].

It should be noted, that the scheme (7) only formally describes real redistribution of a charge in the local surrounding of the ^{57}Fe probe atoms in the $LaCuO_3$ structure. This is proved, in particular, by significant difference between the obtained value of isomer shift (Table 2) which appears to be higher than that earlier obtained for the ferrate $(Ca_{0.50}La_{1.50})Li_{0.50}Fe_{0.50}O_4$

($\delta = -0.19$ mm/s). In the structure of this last ferrate, due to its 2D K_2NiF_4 structure-type each Fe^{4+} cations, stabilized in elongated octahedral oxygen environments, has four electropositive Li cations as the nearest cationic surrounding (Fig. 4(a)) that promotes the formation of strong covalent Fe^{4+}–O^{2-} bonds in the $x0y$ planes. In this case, due to the strong hybridization of 3*d*(Fe) and 2*p*(O) orbitals in the $x0y$ planes, the 3*d* population of Fe^{4+} cations would be improved than that for Fe^{4+} in 3D perovskite $SrFeO_3$ structure (Fig. 4(b)). Nevertheless, so drastic distinction of observable isomer shifts for the $LaCu_{0.99}Fe_{0.01}O_3$ and $(Ca_{0.50}La_{1.50})Fe_{0.50}Li_{0.50}O_4$ oxides cannot be attributed only to the difference of the 3*d* orbitals population of the iron cations. Calculations show that the greatest influence on the isomer shift value is correlated to the 4*s* iron orbital population [32]. In order to evaluate such an effect the following equation (8) given the relation of the ^{57}Fe isomer shift value with electronic populations of the 3*d* and 4*s* orbitals has been used [46]:

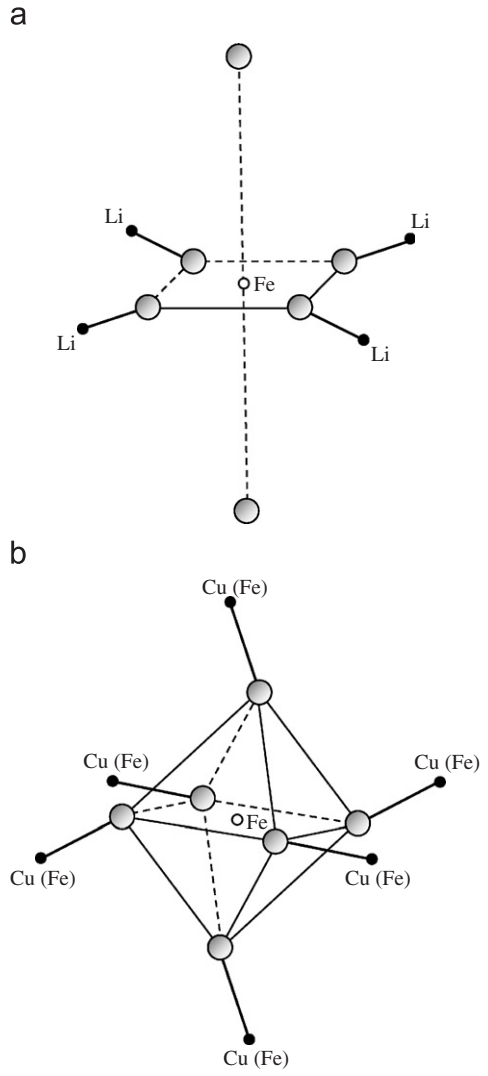

Fig. 4. Schematic representation of anisotropic (Li–O) and isotropic chemical bonding environment for the (FeO_6) octahedra respectively (a) in the 2D K_2NiF_4-type lattice $Ca_{0.5}La_{1.5}Li_{0.5}Fe_{0.5}O_4$ and (b) in the iron-doped 3D perovskite-type $LaM_{0.99}Fe_{0.01}O_3$ (M = Ni, Cu) lattices.

$$\delta = 0.685 + 0.688(n_{3d} - 5) - 1.987 \times n_{4s}, \quad (8)$$

where n_{4s} and n_{3d} are the 4*s* and 3*d* orbitals populations, respectively. To calculate by this equation the 4*s* orbitals population, besides experimental δ value, it is necessary to determine independently 3*d* orbitals population. For this purpose, the values of α_0 and β_0 coefficients entering in Eq. (6) have been calculated. For the actual calculation the charge transfer energy $\Delta = -3$ eV has been used; an estimate of the change in T_σ integral has been made using Harrison's relations $T \sim 1/r^{3.5}$ (where r is M–O distance) [47].

Consequently, the α and β coefficients have been used for the calculations of multi-electronic states $|d^4\rangle$ (Fe^{4+}–O^{2-}) and $|d^5\underline{L}\rangle$ (Fe^{3+}–O^-) contributions in the wave function (Eq. 5) corresponding to the ground state of the iron cations in the formal oxidation state "+4". Further, using the values α and β, the population of 3*d* orbitals, ($n_{3d} = 4\alpha^2 + 5\beta^2$), has been extracted (Table 3). The resulting n_{3d} values and the experimental values of the isomer shift δ for $LaCu_{0.99}Fe_{0.01}O_3$, $SrFeO_3$ and $Ca_{0.50}La_{1.50}Fe_{0.50}Li_{0.50}O_4$ (Table 3) have been substituted in Eq. (8). Consequently the n_{4s} electronic population has been evaluated (Table 3).

Table 3
Isomer shift values (δ_{300K}) of ^{57}Fe Mössbauer spectra (at $T = 300$ K); effectives values of the ligand-to-metal charge transfer energy (Δ_{eff}) and *p*-*d* transfer integral (T_{eff}); ground state of formally tetravalent "Fe^{4+}" ions as a mixing of "ionic" (d^4) and charge-transfer ($d^5\underline{L}$) electronic configurations; 3*d* (n_{3d}) and 4*s* (n_{4s}) electron occupation values

Compound	δ_{300K}, mm/s	Δ_{eff},[a] eV	T_{eff},[a] eV	Ground state	n_{3d}	n_{4s}
$LaCu_{0.99}Fe_{0.01}O_3$ $<r_{Fe-O}> = 1.951(1)$ Å	−0.11	∼−3.0	4.09	$\sqrt{0.34}\|d^4\rangle + \sqrt{0.66}\|d^5\underline{L}\rangle$	4.66	0.27
$SrFeO_3$ $<r_{Fe-O}> = 1.927(5)$ Å	0.05[b]	−3.1	4.27	$\sqrt{0.33}\|d^4\rangle + \sqrt{0.67}\|d^5\underline{L}\rangle$	4.67	0.20
$Ca_{0.5}La_{1.5}Li_{0.5}Fe_{0.5}O_4$ $<r_{Fe-O}> = 1.790$ Å	−0.20[b]	∼−3.0	5.61	$\sqrt{0.37}\|d^4\rangle + \sqrt{0.63}\|d^5\underline{L}\rangle$	4.63	0.32

[a] $\Delta_{eff}(=\Delta-3)$ is defined with respect to the lowest multiplet level of d^4 and $d^5\underline{L}$ configurations (whereas Δ (≈ 0) [48] is defined with respect to the center of gravity of each configurations); $T_{eff} = [3T_\pi^2 + 3T_\sigma^2]^{1/2}$ (where $T_\pi = -0.5$ T_σ, $T_\sigma = 2.20$ eV for $SrFeO_3$ [41]).
[b] These values were taken from [8] and [32].

An analysis of the results of such calculations shows that in case of the 2D ferrate ($Ca_{0.50}La_{1.50}Li_{0.50}Fe_{0.50}O_4$) the n_{3d} population value is slightly lower than that observed for the 3D perovskite $SrFeO_3$. On the contrary the n_{4s} population is slightly improved (Table 3). Such a difference would be attributed to the cationic surrounding of Fe^{4+} in both structures. In the $Ca_{0.50}La_{1.50}Li_{0.50}Fe_{0.50}O_4$ the presence of four "ionic Li–O bonds" as competing bonds in the $x0y$ planes would induce a strong hybridization involving not only empty d_{x2-y2} orbitals but also $4s$ orbitals. For $SrFeO_3$, each (FeO_6) octahedron is surrounding by six Fe–O competing bond. The slight difference between the respective n_{3d} and n_{4s} populations for these two oxides would be attributed both to structural (2D compared to 3D structures) and chemical (Li–O compared to Fe–O as competing bonds) factors.

The ground state of the formally tetravalent "Fe^{4+}" ions derives from the high-spin $t_{2g}^3e_g^1$ (^5E_g electronic term) state that should exhibit or the (cooperative) Jahn–Teller distortion (as in the manganites $RMnO_3$ [49]) or the charge-ordering phenomena (charge disproportionation in the $CaFeO_3$ [10] and $RNiO_3$ [15,16] perovskites). However, the absence in the ^{57}Fe Mössbauer spectra of $LaCu_{0.99}Fe_{0.01}O_3$ noticeable quadrupole interactions (Table 2), and also the presence for iron probe atoms of unique type of the crystallographic positions allows to exclude the local Jahn–Teller distortion of the (FeO_6) polyhedra or the participation of iron probe atoms in the disproportionation process. To explain absence of these effects in the $LaCu_{0.99}Fe_{0.01}O_3$ lattice it would be possible to assume formation in this compound the quarter-filled σ^{*1} band of itinerant e_g electrons which does not lead to the local Jahn–Teller distortion and charge disproportionation (as in the case of $SrFeO_3$ ferrate [12]). However, due to an essential difference in energy for $3d$ orbitals of the Fe^{4+} and Cu^{3+} ions in the $LaCu_{0.99}Fe_{0.01}O_3$ lattice (Fig. 3), the iron probe atoms cannot participate in the formation of a broad σ^{*1} band. This apparent discrepancy can be reconciled taking into account that the ground state of the formally tetravalent "Fe^{4+}" ions in the $LaCu_{0.99}Fe_{0.01}O_3$ perovskite is described by the relatively large occupancy of the $3d^5\underline{L}$ (~64%) configuration and not of the $3d^4$ configuration (~36%) (see Table 3). The $3d$ component of the $3d^5\underline{L}$ configuration is given by the high-spin $t_{2g}^3e_g^2$ ($^6A_{1g}$ ground term) state that inhibits the Jahn–Teller distortion. This indicates that in the case of the Fe^{4+} impurity ions in the $LaCuO_3$ matrix a strong covalency of the Fe–O bonds could eventually quench the local Jahn–Teller distortion of the (FeO_6) polyhedra or charge-ordering phenomena.

4. Conclusions

The comparative Mössbauer study of the $LaM_{0.99}{}^{57}Fe_{0.01}O_3$ perovskites (M = Ni, Cu) has shown that—in spite of both compounds are characterized by the same rhombohedral structure and metallic properties—the electronic states of the ^{57}Fe probe atoms in these matrixes are different.

In the case of $LaNi_{0.99}Fe_{0.01}O_3$, due to the fact that the electronic state of the trivalent nickel ions is dominated by the d^7 configuration corresponding to the ionic "Ni^{3+}–O^{2-}" state, the iron cations are stabilized in the trivalent high-spin $Fe^{3+}(3d^5)$ state with a regular (FeO_6) octahedra. On the contrary, in the case of $LaCu_{0.99}Fe_{0.01}O_3$, the charge transfer equilibrium $Cu^{3+}(d^8)+O^{2-}(p^6)\rightarrow Cu^{2+}(d^9)+O^-(\underline{L})$ is significantly displaced to the right. The dominant $d^9\underline{L}$ ($\approx$70%) ground state, for the (CuO_6) sub-lattice, evaluated through the cluster configuration interaction method, induces in the environment of the iron probe cations a charge transfer $Fe^{3+}+O^-(\underline{L})\rightarrow Fe^{4+}+O^{2-}$, leading to the stabilization of the "Fe^{4+}" state. The comparative analysis of the isomer shift values for "Fe^{4+}" cation in perovskites oxides clearly underlined the influence of the $4s$ orbitals population on the Fe–O bonds character.

Acknowledgments

The authors would like to acknowledge financial support by the Russian Foundation for Basic Research–CNRS (Ref. Nr 05-03-22003), the French Research Agency CNRS (Department of Chemistry - PICS 3200) and the French Ministry for Foreign Affairs for supporting a Thesis in cotutelle by University Bordeaux 1 "Sciences and Technology" and University Lomonosov Moscow (A.B.).

References

[1] B. Buffat, G. Demazeau, M. Pouchard, P. Hagenmuller, Proc. Ind. Acad. Sci. (Chem. Sci.) 93 (1984) 313.
[2] Y. Tanabe, S. Sugano, J. Phys. Soc. Jpn. 9 (1954) 753.
[3] R. Krismamurthy, W.B. Schaap, J. Chem. Educ. 46 (1969) 799.
[4] B. Buffat, G. Demazeau, M. Pouchard, L. Fournès, J.M. Dance, P. Hagenmuller, C.R. Acad, Sci. Ser. II 292 (1981) 509.
[5] Y. Takeda, K. Kanno, T. Takeda, O. Yamamoto, M. Takano, N. Nakayama, Y. Bando, J. Solid State Chem. 63 (1986) 237.
[6] F. Kanamuru, H. Miyamoto, Y. Mimura, M. Koizumi, Mater. Res. Bull. 5 (1970) 257.
[7] J.B. MacChesney, R.C. Sherwood, J.F. Potter, J. Chem. Phys. 43 (1965) 1907.
[8] G. Demazeau, N. Chevreau, L. Fournès, J.L. Soubeyroux, Y. Takeda, M. Thomas, M. Pouchard, Rev. Chim. Miné. 20 (1983) 155.
[9] G. Demazeau, B. Buffat, M. Pouchard, P. Hagenmuller, Z. Anorg. Allg. Chem. 491 (1982) 60.
[10] M. Takano, N. Nakanishi, Y. Takada, S. Naka, T. Takada, Mater. Res. Bull. 12 (1977) 923.
[11] M. Takano, S. Nasu, T. Abe, K. Yamamoto, S. Endo, Y. Takeda, J.B. Goodenough, Phys. Rev. Lett. 67 (1991) 3267.
[12] Y. Takeda, S. Naka, M. Takano, J. Phys. 40 (1979) C2–C331.
[13] T. Takeda, S. Komura, H. Fujii, J. Magn. Magn. Mater. 31-34 (1983) 797.
[14] J.-C. Grenier, N. Ea, M. Pouchard, Mater. Res. Bull. 19 (1984) 1301.
[15] J.A. Alonso, J.L. Garcia-Munoz, M.T. Fernandez-Diaz, M.A.G. Aranda, M.J. Martinez-Lope, M.T. Casais, Phys. Rev. Lett. 82 (1999) 3871.
[16] J.A. Alonso, M.J. Martinez-Lope, M.T. Casais, J.L. Garcia-Munoz, M.T. Fernandez-Diaz, Phys. Rev. B 61 (2000) 1756.

[17] I.I. Mazin, D.I. Khomskii, R. Lengsdorf, J.A. Alonso, W.G. Marshall, R.M. Ibberson, A. Podlesnyak, M.J. Martinez-Lope, M.M. Abd-Elmeguid, Phys. Rev. Lett. 98 (2007) 176406.
[18] S.-J. Kim, G. Demazeau, I. Presniakov, K. Pokholok, A. Sobolev, D. Pankratov, N. Ovanesyan, J. Am. Cer. Soc. 123 (2001) 8127.
[19] S.-J. Kim, G. Demazeau, I. Presniakov, K. Pokholok, A. Baranov, A. Sobolev, D. Pankratov, N. Ovanesyan, Phys. Rev. B 66 (2002) 014427.
[20] I. Presniakov, G. Demazeau, A. Baranov, A. Sobolev, K. Pokholok, Phys. Rev. B 71 (2005) 054409.
[21] F. Bertaut, F. Forrat, J. Phys. Radium 17 (1956) 129.
[22] A. Wold, B. Post, E. Banks, J. Am. Chem. Soc. 79 (1957) 4911.
[23] M. Foex, A. Mancheron, M. Line, C. R. Acad. Sci. 250 (1960) 3027.
[24] G. Demazeau, C. Parent, M. Pouchard, P. Hagenmuller, Mater. Res. Bull. 7 (1972) 913.
[25] N. Hamada, J. Phys. Chem. Solids 54 (1993) 1157.
[26] J.B. Goodenough, N.F. Mott, M. Pouchard, G. Demazeau, Mater. Res. Bull. 8 (1973) 647.
[27] F. Yill, Y. Gros, F. Hartmann-Bourton, P. Strobel, J.L. Tholence, A. Sulpice, Hyperfine Inter. 93 (1994) 1705.
[28] G. Demazeau, A. Baranov, G. Heymann, H. Huppertz, A. Sobolev, I. Presniakov, Solid State Sci. 9 (2007) 376.
[29] D.B. Currie, M.T. Weller, Acta Crystallogr. C 47 (1991) 696.
[30] C. Weigl, K.J. Range, J. Alloys Compds. 200 (1993) L1.
[31] R.D. Shannon, Acta Crystallogr. A 32 (1976) 751.
[32] F. Menil, J. Phys. Chem. Solids 46 (1985) 763.
[33] J.B. Torrance, J. Solid State Chem. 96 (1992) 59.
[34] W.C. Martin, L. Hagan, J. Reader, J. Sugar, J. Phys. Chem. Ref. Data. 3 (1974) 771.
[35] J. Zaanen, G.A. Sawatzky, J.W. Allen, Phys. Rev. Lett. 55 (1985) 418.
[36] J. Zaanen, G.A. Sawatzky, J. Solid State Chem. 88 (1990) 8.
[37] G. Van der Laan, B.T. Thole, G.A. Sawatzky, R. Karnatak, J.-M. Esteva, Phys. Rev. B 33 (1986) 4235.
[38] Z. Hu, G. Kaindl, S.A. Warda, D. Reinen, F.M.F. de Groot, B.G. Muller, Chem. Phys. 232 (1998) 63.
[39] T. Mizokawa, A. Fujimori, T. Arima, Y. Tokura, N. Mori, J. Akimitsu, Phys. Rev. B 52 (1995) 13865.
[40] T. Mizokawa, A. Fujimori, N. Namatame, K. Akeyama, N. Kosugi, Phys. Rev. B 49 (1994) 7193.
[41] R. Iczkowski, J. Margrave, J. Am. Chem. Soc. 83 (1961) 3547.
[42] A.W. Webb, K.H. Kim, C. Bouldin, Solid State Commun. 79 (1991) 507.
[43] J.H. Choy, D.K. Kim, S.H. Hwang, G. Demazeau, Phys. Rev. B 50 (1994) 16631.
[44] T. Mizokawa, A. Fujimori, N. Namatame, Y. Takeda, M. Takano, Phys. Rev. B 57 (1998) 9550.
[45] S. Darracq, S. Matar, G. Demazeau, Solid State Commun. 85 (1993) 961.
[46] R. Ingalls, A. Van der Woude, G. A. Sawatzky, Mössbauer Isomer Shifts, in: G. K. Shenoy, F. E. Wagner (Eds.), North Holland, Amsterdam, 1978, Chapter 7.
[47] W.A. Harrison, Electronic Structure and the Properties of Solids, Freeman, San Francisco, 1980.
[48] A.E. Bocquet, A. Fujimori, T. Mizokawa, T. Saitoh, H. Namatame, S. Suga, N. Kimizuka, Y. Takeda, M. Takano, J. Phys. Rev. B 45 (1992) 1561.
[49] J.B. Goodenough, Magnetism and the Chemical Bond, Interscience-Wiley, New York, 1963.